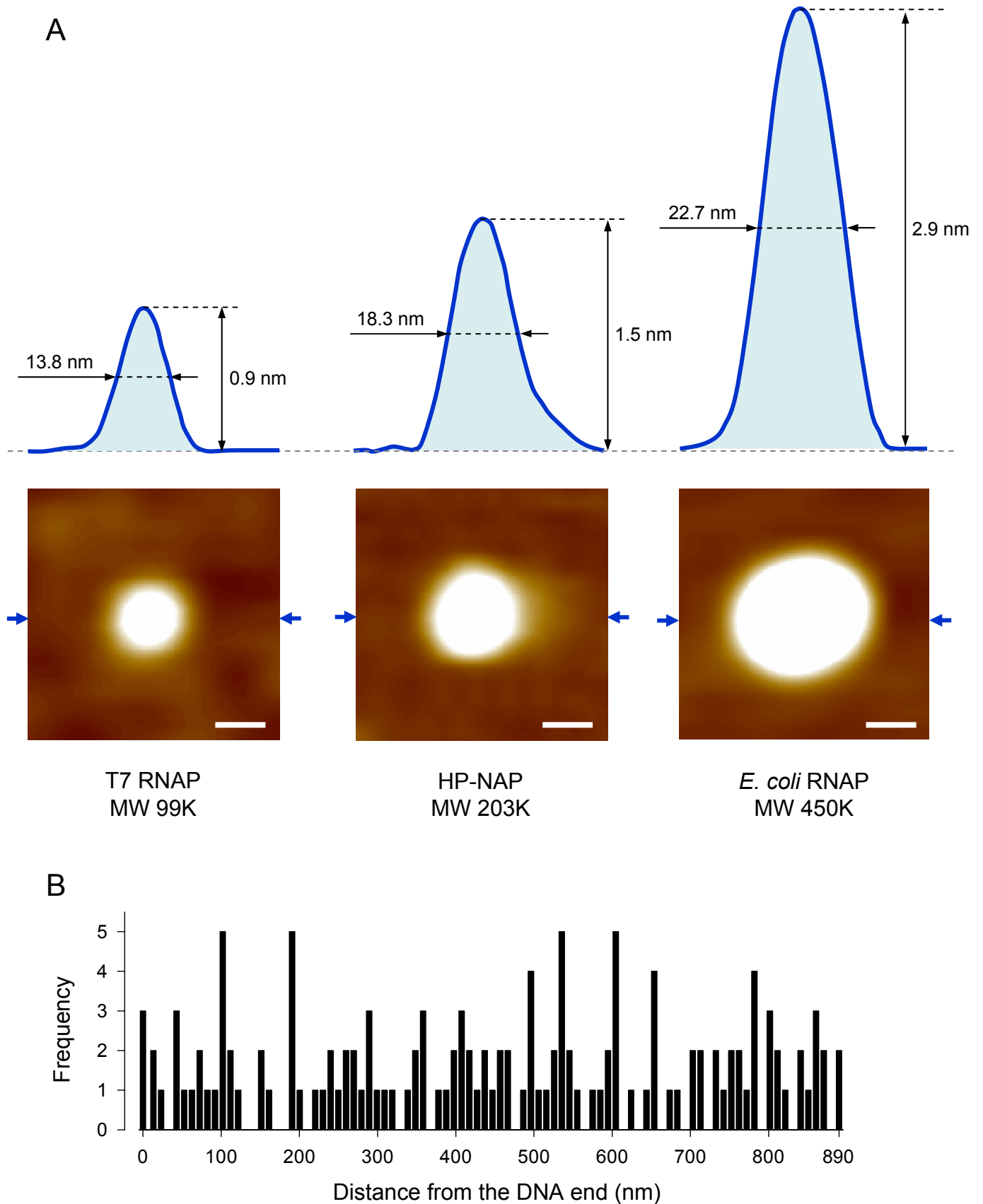
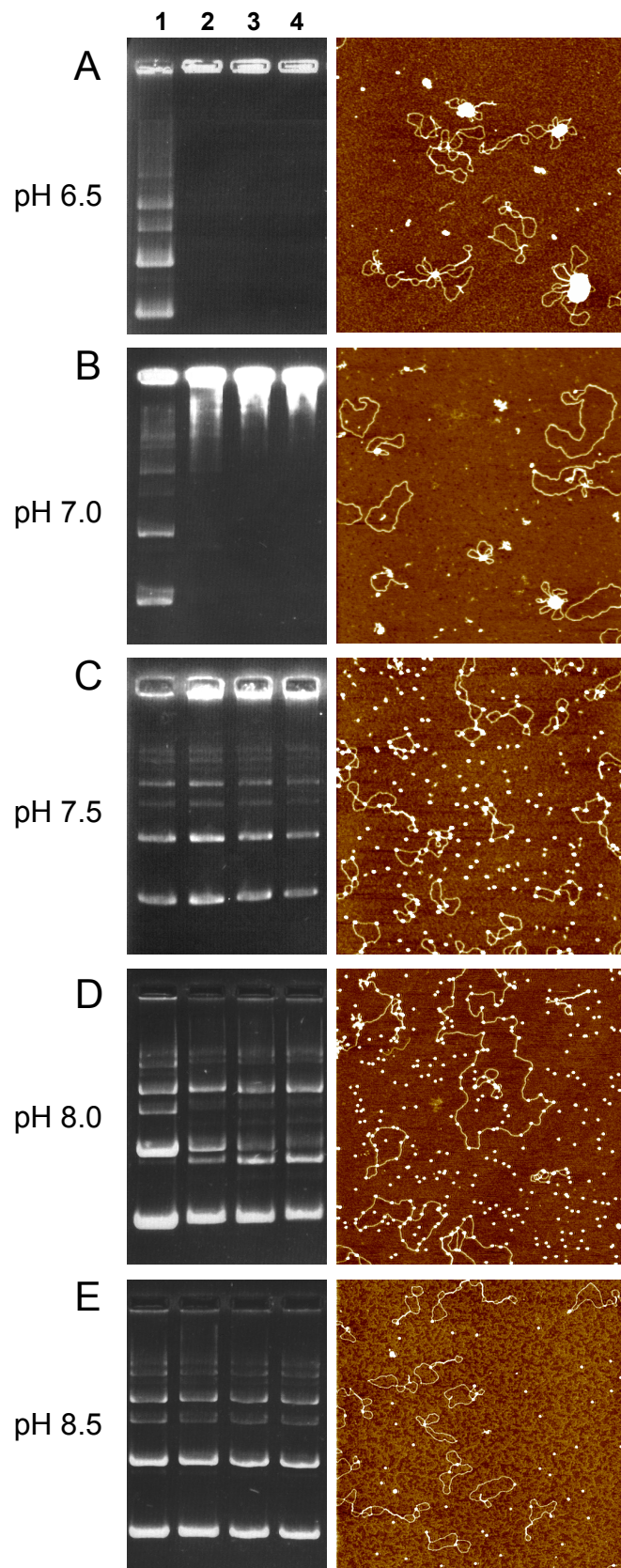


**Figure 1 Supplementary.** Molecular surface of HP-NAP. The positively charged residues are depicted in blue, the negatively charged ones in red. Pictures were generated with the program Pymol (32) using the coordinates deposited at the RCSB Protein Data Bank with accession code 1JI4.



**Figure 2 Supplementary.** Molecular size comparison of proteins with different molecular weight and HP-NAP distribution along the DNA. A) Images of T7 RNA polymerase, HP-NAP and *E. coli* RNA Polymerase (bottom) and corresponding cross-section profiles in the direction of the blue arrows (top). Scale bar 50 nm. B) The bar-plot represents the frequency of HP-NAP binding at different positions along the 890 nm long DNA fragment at pH 7.5. Each bar corresponds to a DNA region of 10 nm.



**Figure 3 Supplementary.** DNA gel retardation assays (left panels) and AFM images (right panels) of HP-NAP-DNA complexes at different pH values. A) pH 6.5; B) pH 7.0; C) pH 7.5; D) pH 8.0; E) pH 8.5. In all gels, *lane 1* refers to supercoiled plasmid DNA alone (20 nM), *lanes 2-4* to plasmid DNA with HP-NAP at a molar ratio of 1:15, 1:30 and 1:60, respectively. The different bands denote different DNA topoisomers. The large white globular features in the AFM images of panels A and B represent HP-NAP-DNA aggregates involving one or few plectonemes and many HP-NAP dodecamers. The white dots in the AFM images of panels C, D and E represent single HP-NAP dodecamers. Agarose gels were stained with ethidium bromide. In all AFM images the scan size is 2  $\mu\text{m}$ .

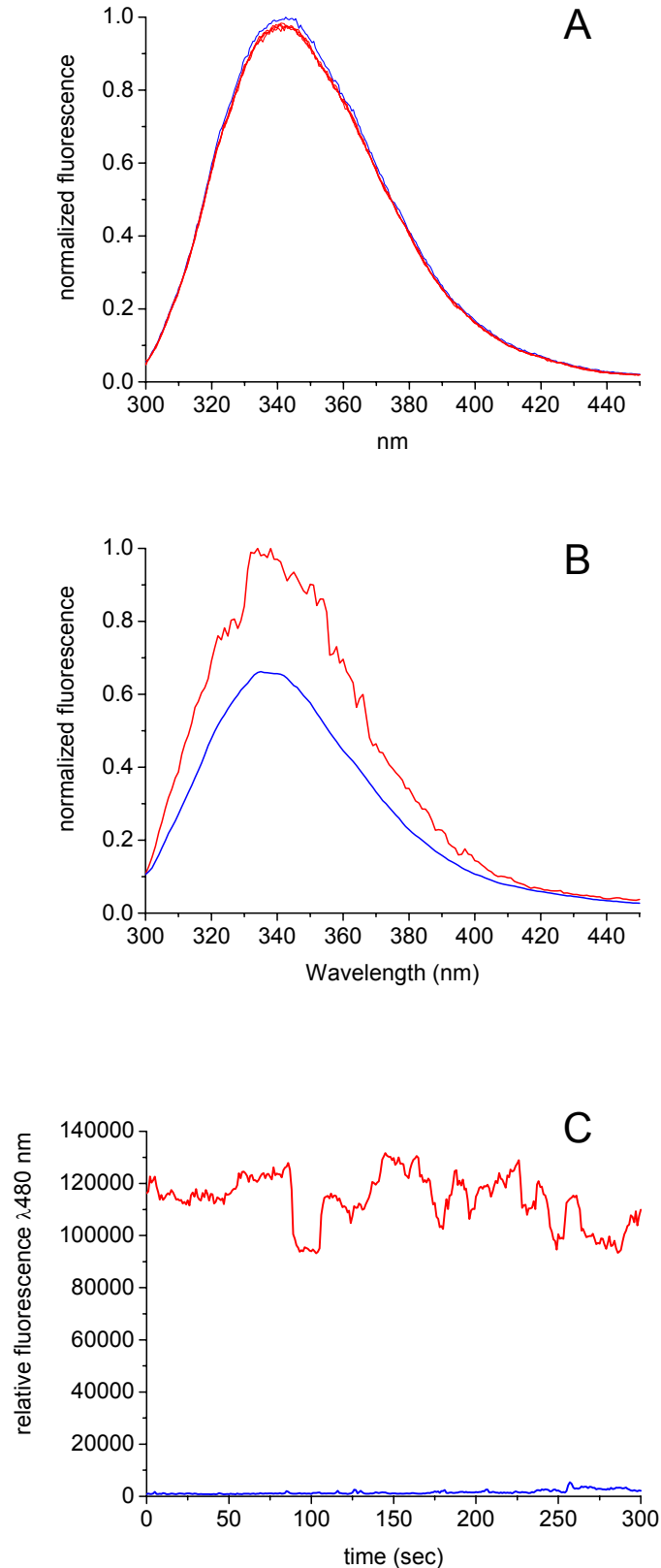


**Figure 4 Supplementary.** Fluorescence emission spectra of HP-NAP incubated with linearized plasmid DNA at different pH values. Panel A, emission spectra of 0.5  $\mu\text{M}$  HP-NAP at pH 8.5 before (blue line) and after 4 additions of 0.5 nM DNA (red lines). Panel B, emission spectra of 0.5  $\mu\text{M}$  HP-NAP at pH 6.5 before (blue line) and after addition of 0.5 nM DNA (red line). Panel C, 90° light scattering of 0.5  $\mu\text{M}$  HP-NAP at pH 6.5 before (blue line) and after addition of 0.5 nM DNA (red line). Light scattering was measured with both excitation and emission wavelength set at 480 nm to check for the presence of aggregated particles.

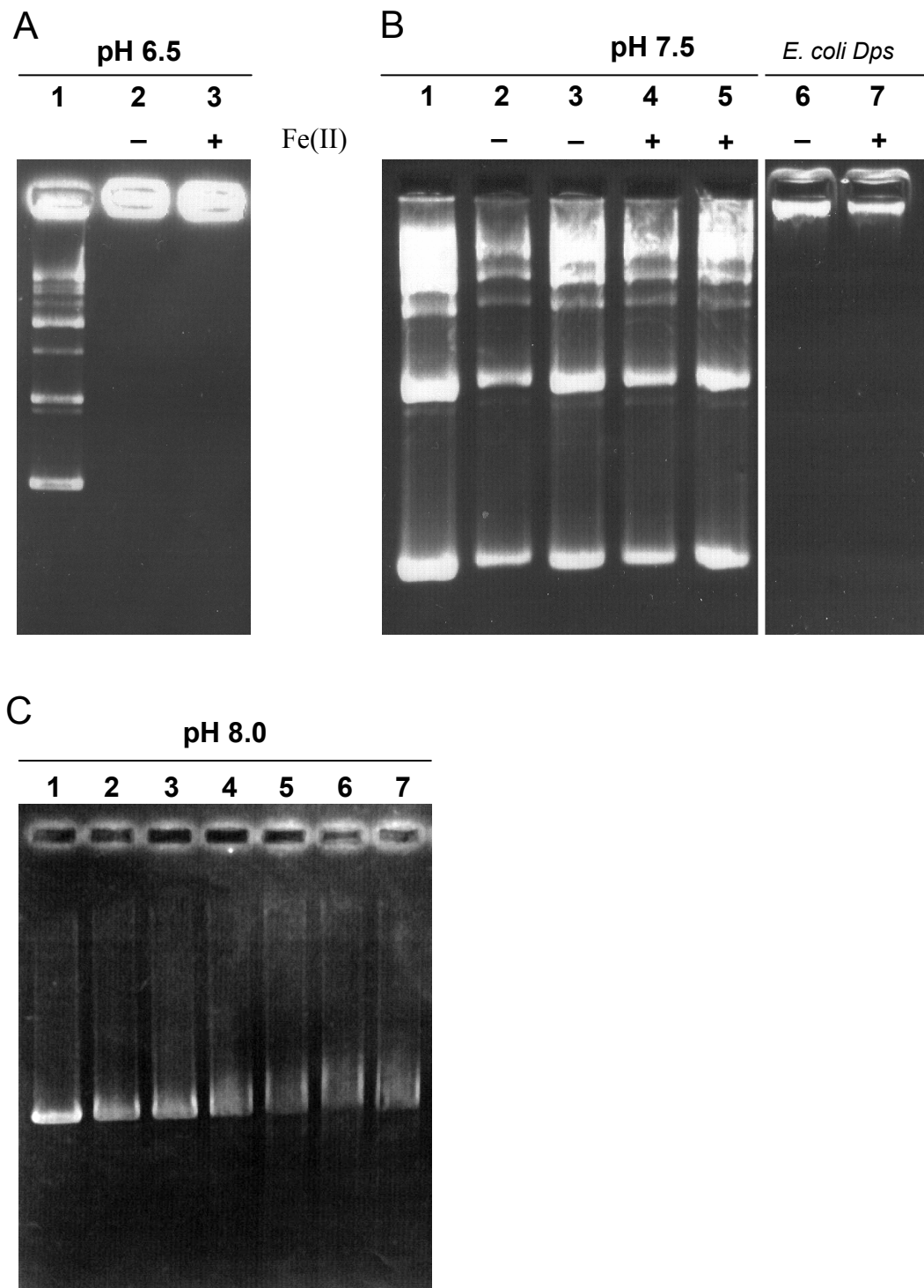


**Figure 5 Supplementary.** Effect of iron-loading on the DNA binding ability of HP-NAP (A, B) and determination of the HP-NAP- linearized DNA binding stoichiometry at pH 8.0 (C). In all experiments DNA was 20 nM. A) Effect of iron-loading at pH 6.5. Lane 1, plasmid DNA alone. Lanes 2-3, plasmid DNA plus apo-HP-NAP (lane 2) and plus Fe-loaded HP-NAP (lane 3), protein:DNA molar ratio 15:1. B) Effect of iron-loading at pH 7.5. Lane 1, plasmid DNA alone. Lanes 2-7, plasmid DNA plus apo-HP-NAP, protein:DNA molar ratio 30:1 (lane 2) and 15:1 (lane 3); plasmid DNA plus Fe-loaded HP-NAP, protein:DNA molar ratio 30:1 (lane 4) and 15:1 (lane 5); plasmid DNA plus *E. coli* apo-Dps (lane 6) and plus Fe-loaded *E. coli* Dps (lane 7), protein:DNA molar ratio 15:1. D) Binding stoichiometry at pH 8.0. Lane 1, DNA alone. Lanes 2-7, DNA plus HP-NAP; protein:DNA molar ratios: 25:1 (lane 2); 50:1 (lane 3); 100:1 (lane 4); 200:1 (lane 5); 400:1; (lane 6); 800:1 (lane 7). Saturation is achieved upon addition of 8.0  $\mu$ M HP-NAP (lane 6). Agarose gels stained with ethidium bromide.

**Supplementary Table I.** Effect of HP-NAP and *E. coli* Dps on Fe(II)-dependent hydroxyl radical formation

	Protein Concentration nM	Degradation inhibition <sup>a</sup> %
HP-NAP	50	53.4 ± 2.6
	200	69.8 ± 2.1
	400	72.9 ± 3.1
<i>E. coli</i> Dps	50	51.8 ± 3.5
	200	68.3 ± 2.4
	400	71.1 ± 2.1

<sup>a</sup> The values are the mean ± standard deviation for experiments carried out in triplicate